

Luminescence studies of plasma-deposited hydrogenated silicon

R. A. Street, J. C. Knights, and D. K. Biegelsen

Xerox Palo Alto Research Center, Palo Alto, California 94304

(Received 13 March 1978)

The photoluminescence of plasma-deposited amorphous silicon is investigated. The luminescence intensity and spectral line shape are shown to be sensitive to many deposition variables, in particular the power coupled into the discharge, the concentration of silane in the gas stream, and the deposition substrate temperature. Maximum intensity is obtained in samples deposited with low power (~ 1 W), a silane concentration of $\geq 10\%$ and a deposition temperature of 200–300°C. ESR studies show that the luminescence intensity is determined by competing nonradiative transitions to localized defect states whose density varies with deposition conditions. The presence of defect states is related to the way hydrogen is incorporated into the samples, but the details of the defect structure are not yet clear. Oxygen impurities are observed to give a broad, weak luminescence peak centered near 1.1 eV. It is suggested that the active oxygen centers are similar to the charged defects postulated for chalcogenide glasses.

I. INTRODUCTION

The structure and electronic properties of amorphous tetrahedral semiconductors are well-known to be sensitive to sample preparation conditions. In evaporated or sputtered films, the most important variable is the temperature of deposition or of annealing,¹ but the rate and angle of deposition also have significant effects.² The use of a low-pressure plasma to decompose silane results in amorphous films whose electronic properties differ greatly from evaporated or sputtered Si.³ Undoubtedly, the most important factor in this case is the incorporation of hydrogen, which is present in concentrations sometimes as large as 50 at.%.⁴ Indeed, in view of the large hydrogen concentration, the validity of comparing the two types of samples is questionable. Hydrogen seems to be responsible for an increase in the band gap of the material.⁵ However, apart from its ability to reduce the density of localized states in the gap, the influence of hydrogen on the transport and recombination mechanisms is not yet clearly understood.

Luminescence measurements have established that the structure and electronic properties of plasma-deposited films are also sensitive to preparation conditions.^{6,7} Raising the temperature of deposition or annealing appears to have an effect similar to that in evaporated Si, decreasing the density of localized gap states, and a corresponding increase in luminescence intensity is observed.⁶ The influence of other deposition parameters has not been reported, and there is a tacit assumption in the literature that samples produced by different groups can be compared directly. In view of the complexity of the plasma-deposition process, and the fact that at least two radically different methods of constructing the deposition reactor have been used, it is important to verify

this assumption. This paper, therefore, has two main objectives. Firstly, it includes a survey of the influence on the luminescence of a wide range of deposition parameters—rf power, gas concentration, substrate temperature, gas pressure, bias voltage, etc.—to determine, in a phenomenological way, the deposition variables which must be controlled to obtain well defined and reproducible films. These results are presented in Sec. III along with the luminescence properties of oxygen impurities and ESR measurements of the spin density. We demonstrate that, at least from the point of view of luminescence, other deposition parameters are as important as the substrate temperature. The variation in luminescence intensity when the deposition parameters are changed is caused by competing nonradiative transitions through localized states at defects. Thus the second objective is to investigate these localized states in the gap. We show that there is a correlation between the luminescence intensity and the ESR spin density, which also measures the localized state density. The ability to create samples of widely differing densities of defects, by varying the deposition conditions, allows us to demonstrate this correlation. Apparently the properties of the defects are independent of which deposition variable is changed. Finally, it is shown that a model derived from luminescence decay time data explains in detail the relation between luminescence intensity and ESR.

II. EXPERIMENTAL DETAILS

A. Sample preparation

The plasma reactor used in this work is shown schematically in Fig. 1. The 13.56-MHz rf power is coupled into the plasma capacitatively via the cathode C and an L -section matching network.

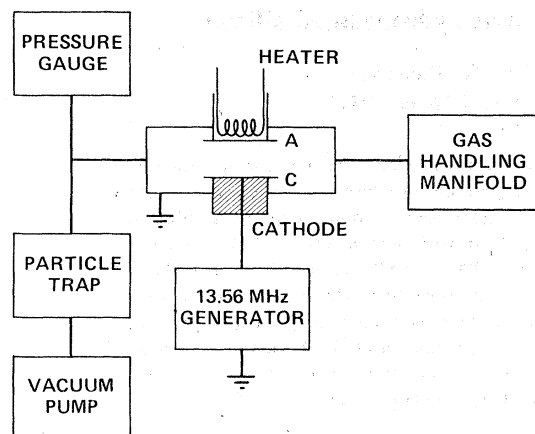


FIG. 1. Schematic diagram of the reactor for the glow discharge decomposition of silane.

Samples are clamped to the anode A. The surface area of the cathode is $\sim 13 \text{ cm}^2$ and the volume of the reaction zone is $\sim 150 \text{ cm}^3$. For the majority of the work described here, the anode A was electrically connected to the metal reactor wall and held at ground potential. With this arrangement, the system is an asymmetric plate area capacitor and, because of the different electron and ion mobilities, the cathode self-biases to a negative dc potential. The effects of bias on the growing surface were investigated using a separate rf supply and matching network to feed power through the anode. Both rf supplies were driven from a common oscillator to maintain a fixed phase relationship between the two electrodes.

The sample temperature in either configuration can be varied between 25°C and $\sim 450^\circ\text{C}$ and held constant over a typical deposition time (1 h) to $\pm 1^\circ\text{C}$.

The parameters varied in these experiments were (i) concentration of SiH_4 in SiH_4 -Ar mixtures (100%–0.1%); (ii) rf power (0.5–40 W net input); (iii) substrate temperature T_s (25 – 400°C); (iv) bias voltage (0–40 V); and (v) Pressure (0.05–0.24 Torr). Pressure variations were achieved by reducing the flow rate or by throttling the vacuum pump. The changes in flow rate were not recorded.

In all the data shown, the values of the silane concentration and rf power are stated explicitly. Unless otherwise noted, the remaining parameters were held at standard values, namely, anode deposition (zero bias), $T_s = 230^\circ\text{C}$, pressure = 0.15 Torr, flow rate = 140 sccm (standard cubic centimeter per minute).

B. Luminescence measurements

The luminescence measurements were performed on samples usually held at $\sim 10 \text{ K}$. The samples were deposited on ground-glass sub-

strates to remove interference effects. The excitation source was the 5145-Å line of an argon laser, and the luminescence was normalized to the excitation intensity. Throughout the investigation the same monochromator resolution (0.015 eV) and detector (cooled PbS) were used, so that the luminescence intensity of different samples could be compared reliably. The luminescence spectra were corrected for the response of the detection system, which was determined using a tungsten lamp of known color temperature. This procedure was not used in our earlier work⁸ and the peaks of the corrected spectra are about 0.07 eV higher in energy than had been reported. The excitation intensity was kept approximately constant for different samples to minimize possible intensity dependence of the spectrum. Furthermore, an experimental arrangement was used that allowed six samples to be compared under identical conditions. A possible source of error in comparing intensities is incomplete absorption of the excitation light. In a few cases, when low rf power and very low silane concentrations were used, the deposition rate was so low that the samples were only 1000–3000 Å thick, and the luminescence intensity may have been underestimated. These samples are noted in the discussion of results.

Approximately 100 samples were investigated, the majority of which had different deposition conditions. However, in samples deposited under nominally the same conditions, the luminescence intensity and spectral shape were found to be essentially identical, indicating that the deposition was well controlled and the conditions accurately repeatable. The only exception was the luminescence peak at 1.1 eV which is believed to be due to oxygen impurities as described below.

III. RESULTS

A. Dependence on deposition power and silane concentration

The rf power and silane concentration have pronounced effects on the luminescence properties. In general, the luminescence intensity of anode samples increases with decreasing power and with increasing silane concentration, and a corresponding change in the luminescence spectrum occurs. Figure 2 shows representative luminescence spectra for samples with different power and gas concentrations. (The concentration is defined as the volume percentage of silane in the silane-argon mixture.) In each case, the main luminescence peak is near 1.4 eV, although there are systematic variations of about 0.1 eV around this energy. The shape of the spectra also varies with deposition conditions. Both effects are seen clearly in Fig. 2(b) for 10% samples of different rf power. As

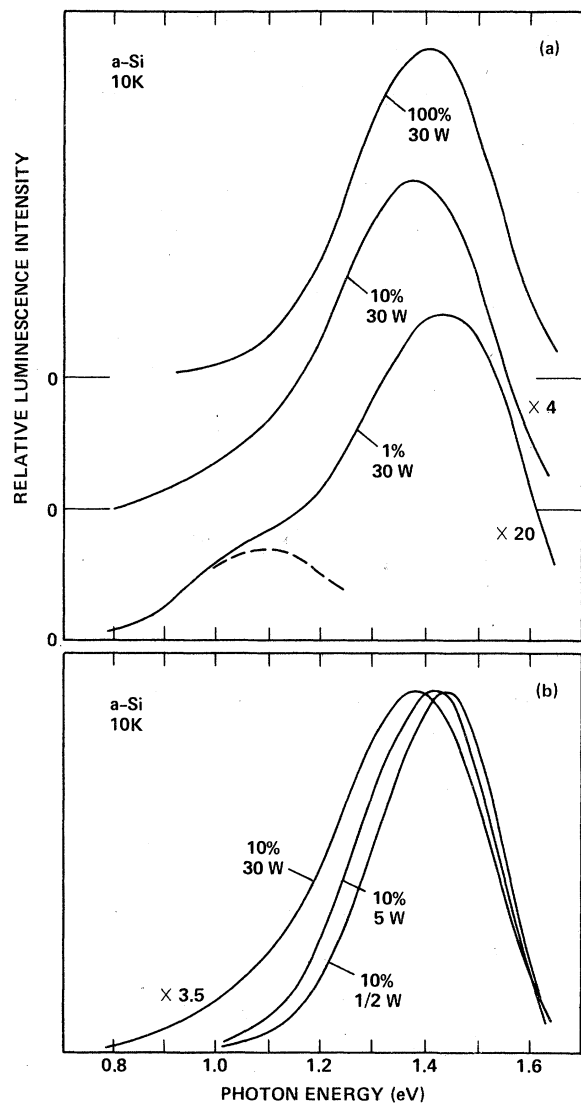


FIG. 2. (a) Luminescence spectra of *a*-Si samples deposited at 30-W rf power and different gas concentrations. The dashed line represents the shape of the luminescence peak responsible for the low-energy shoulder to the spectrum. (b) Luminescence spectra for samples with the same gas concentration (10%) but different power.

the power increases the spectrum broadens and the peak shifts to lower photon energy.

Figure 2(a) shows that in 1% 30-W samples there is an additional peak centered at ~1.1 eV which is observed as a shoulder on the low-energy side of the main peak. This feature was usually present in low concentration samples, particularly those deposited at high power. However, its occurrence was not always reproducible, and in a few samples its intensity was much reduced. This observation suggests that the peak originates from

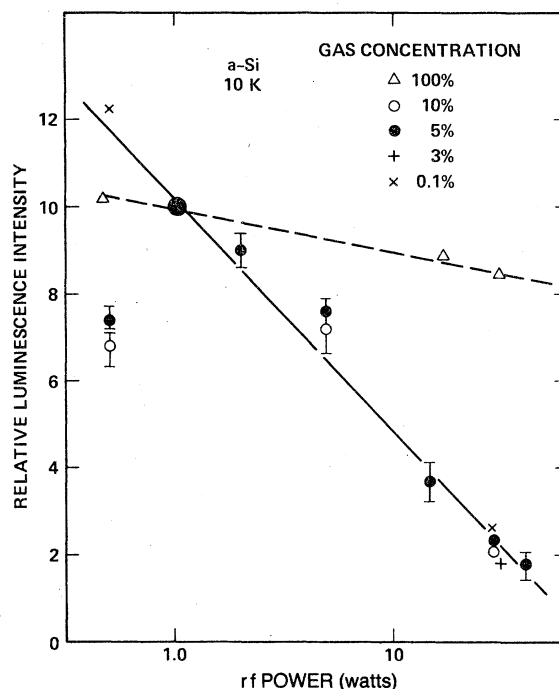


FIG. 3. Relative change in luminescence intensity with deposition power. For each gas concentration the intensities are normalized to the value at 1 W. The variation with gas concentration is shown in Fig. 4.

an impurity in the deposition, and further evidence for this view is given in Secs. III E and III F.

The relation between the intensity of the luminescence and rf power is shown in Fig. 3 for samples of widely differing silane concentration. For each concentration, the intensities are normalized to the value in 1-W samples. With the exception of 100% silane, the intensity decreases with the same logarithmic dependence on power between 1 and 40 W, with a total change of about a factor of 6. The 1/2-W samples of 5% and 10% samples depart from this relation. However, these samples were particularly thin and incomplete absorption of the excitation light may be partially responsible for the result. The 100% samples also deviate from the usual behavior and exhibit a very weak power dependence.

In Fig. 4, the intensity of the luminescence is plotted against silane concentration at two different values of the rf power. In general, the intensity increases proportionally to the square root of silane concentration. However, in 1-W samples, the intensity saturates above 10%, and this effect obviously corresponds to the different power dependence of the 100% samples seen in Fig. 3. It is apparent from Fig. 4 that over the investigated range of power and gas concentration, the intensity of the luminescence changes by two or

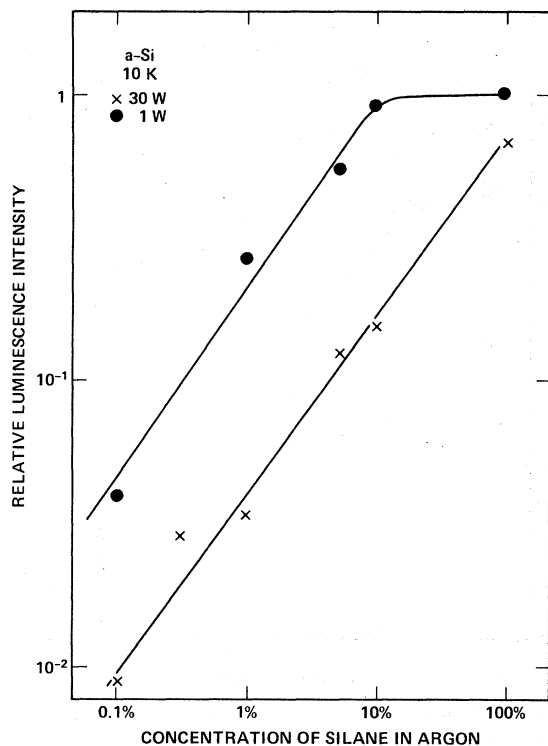


FIG. 4. Variation of luminescence intensity with gas concentration for two values of rf power (1 W and 30 W).

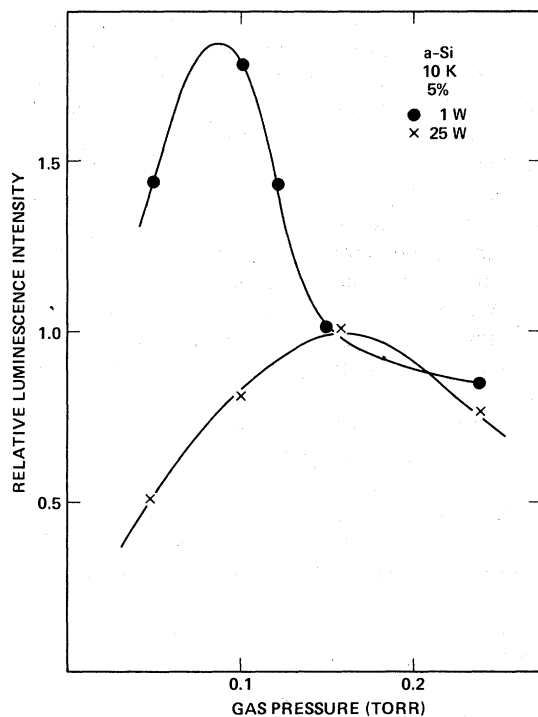


FIG. 5. Relative variation of luminescence intensity with total gas pressure for samples with a gas concentration of 5% and two different rf powers. The intensities are normalized to the value at 0.15 Torr.

ders of magnitude, which demonstrates the sensitivity of the sample structure to these deposition parameters.

B. Dependence on gas pressure

Figure 5 illustrates the influence of the total gas pressure in the reactor on the luminescence intensity. The data are shown for two values of the rf power and are normalized to the value at 0.15 Torr. It is observed that the peak intensity of the high-power samples occurs near 0.15 Torr whereas in the 1-W samples the peak occurs at a substantially lower pressure. Possibly the different behavior is related to the deposition rate properties discussed in Sec. IV. C. Thus, the 25-W sample is in the silane-depleted regime, where the deposition is supply limited, and decreasing the pressure will increase the degree of depletion. However, the 1-W sample is not depleted at 0.15 Torr, but may be at substantially lower pressure.

C. Dependence on substrate temperature and annealing

Both Engemann and Fischer⁶ and Pankove and Carlson⁹ report that the luminescence intensity increases with substrate temperature T_s or annealing up to about 300 °C. Figure 6 shows the dependence of luminescence intensity on T_s for our 1-W and 25-W samples, at 5% concentration. The general behavior is in agreement with the previous data, but it is seen that the 1-W samples have a much stronger dependence on substrate temperature than 25-W samples. Part of the additional intensity in the latter at low T_s may be due to additional peaks at low energy since the spectra

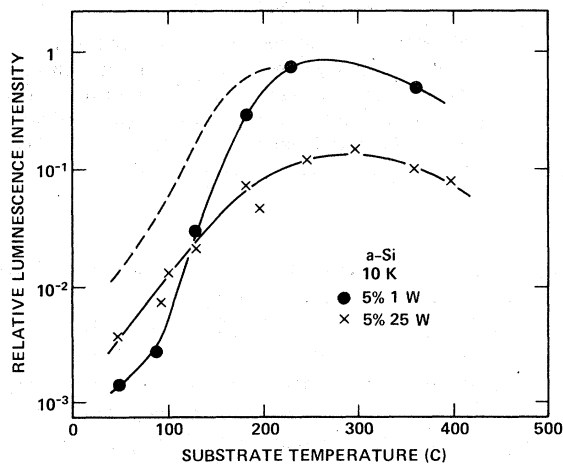


FIG. 6. Dependence of the luminescence intensity on substrate temperature for 1-W and 25-W samples of 5% concentration. The dashed line illustrates the dependence observed by Ref. 6.

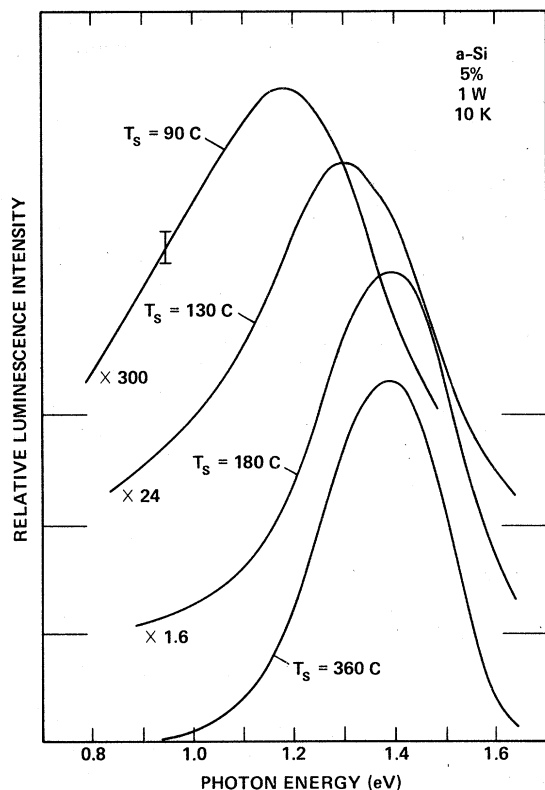


FIG. 7. Luminescence spectra for the various indicated substrate temperatures, T_s .

are particularly broad. Above 300 °C the intensity begins to decrease as was also observed in annealing experiments by Pankove and Carlson⁹ who attribute the effect to the removal of hydrogen from the film.

Figure 7 shows the luminescence spectra at different substrate temperatures. At low temperature, the peak becomes broad and shifted to low energy. Although Engemann and Fischer⁶ reported a similar effect, we do not observe the specific additional luminescence peaks that they found near 1.1 eV and 0.9 eV. Instead there is a broad featureless luminescence band. Between about 200 and 400 °C the spectra are similar with only a small additional low-energy broadening in the lower-temperature samples.

Engemann¹⁰ also found that annealing a film deposited at low temperature enhances the luminescence and reproduces the spectrum of a high-temperature deposition. Figure 8 shows data for a 50 °C deposited sample which is annealed at 150 and 250 °C, and a large increase in luminescence intensity occurs. However, the spectral shape of the annealed film is significantly different from that of samples deposited at 230 °C. The main peak is centered at 1.3 eV instead of 1.45 eV. Thus, it appears that in our samples annealing does not

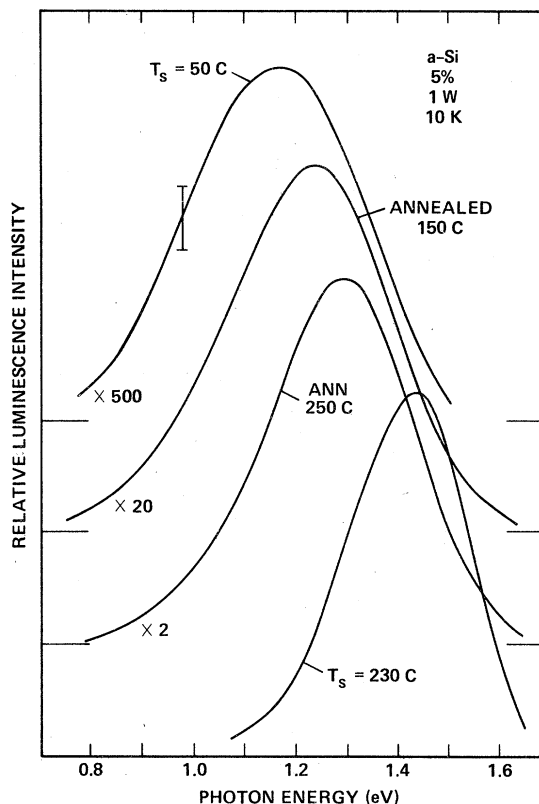


FIG. 8. Luminescence spectra of a sample deposited at 50 °C, showing the effect of annealing at 150 and 250 °C. Also shown for comparison is the spectrum of a sample deposited at 230 °C.

completely reproduce the effect of a high substrate temperature.

D. Dependence on bias voltage

As described in Sec. II., rf power can be fed into the discharge through the anode, thereby producing a negative dc bias on the sample surface. This bias is approximately proportional to power and for the geometry used is -40 V when 30 W of power is being coupled through the anode. Since the electrical asymmetry is now reversed, we term these "cathode" samples. Figure 9 shows luminescence spectra as a function of rf power. There are two significant changes in the luminescence of these samples compared to anode-deposited ones. Firstly, the luminescence intensity varies by less than 20% with deposition power between 1 and 30 W, compared to a factor 5 in anode samples, and the absolute intensity is similar to the 1-W anode samples. Secondly, the spectra are shifted to low energy by about 0.07 eV compared to anode samples of the same deposition conditions. However, a similar broadening of the spectra at high power is observed as was shown in Fig. 2(b).

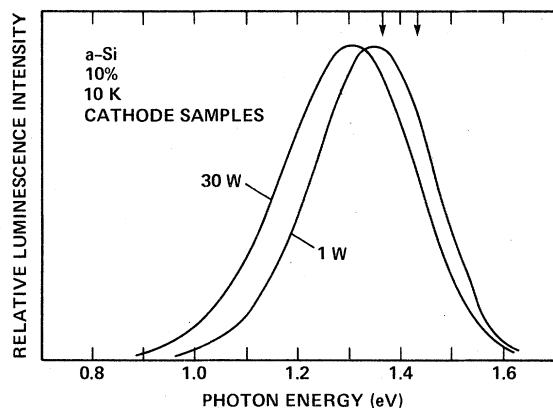


FIG. 9. Luminescence spectra of cathode samples which are deposited under conditions of substantial bias voltage with respect to the plasma. The arrows indicate the energy of the luminescence peak in equivalent anode samples (right arrow 1 W; left arrow 30 W).

The peak of the spectra of our anode samples is at higher energy than was found by other groups, particularly Engemann and Fischer^{6,7} who report an energy of 1.25 eV. Since bias is found to shift the peak of lower energy, it is possible that the structure of our cathode samples is closer to the type of sample investigated by Engemann and Fischer. However, as one test of this hypothesis,

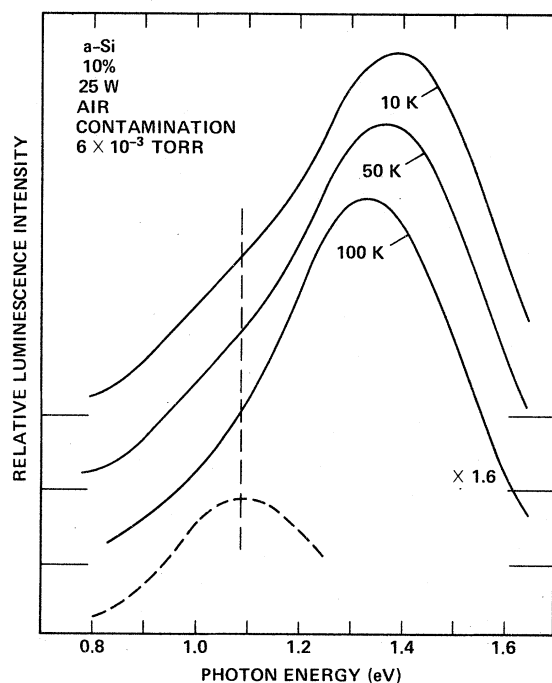


FIG. 10. Luminescence spectra at different temperatures of a sample deposited with the reactor contaminated with a low partial pressure of air. The dashed line reproduces the low-energy luminescence peak shown in Fig. 2(a).

we have investigated cathode samples deposited at low substrate temperatures and subsequently annealed. The results are similar to those obtained on anode samples (Fig. 9) except that the luminescence peaks are 0.05–0.1 eV lower in energy. No evidence of structure is observed in the spectra, in contrast to observation by Engemann and Fischer on samples under similar conditions. We conclude therefore that our cathode samples do not completely reproduce the structure of their films.

E. Effects of gas impurities: an oxygen peak at 1.1 eV

The plasma-deposition process, like evaporation and sputtering, suffers from the disadvantage that the residual gas in the chamber may introduce active impurities into the samples. To investigate atmospheric impurities, both air and pure nitrogen were introduced into the reactor during deposition. A pressure of $\sim 10^{-2}$ Torr nitrogen was found to have no detectable effect on the shape or intensity of the luminescence spectrum. However, a similar pressure of air resulted in the spectra shown in Fig. 10. At 10 K, there is a pronounced shoulder on the low-energy side of the main peak, which is quenched more rapidly with temperature than the 1.4-eV peak. From the absence of any effect of nitrogen, we deduce that oxygen is an active impurity in α -Si. Infrared measurements also confirm that oxygen bonded to Si is present in substantial quantities in these films.

Also shown in Fig. 10 is the low-energy peak centered near 1.1 eV which is found in low-concentration samples and which is reproduced from Fig. 2(a). The similarity between this peak and the one introduced by oxygen is obvious, and suggests that the two lines may be identical. Figure 11 shows the temperature dependence of the 1% 30-W sample, and it is seen that thermal quenching of the 1.1-eV peak occurs at a lower temperature than for the 1.4-eV peak. A comparison between Figs. 10 and 11 shows that the peaks at 1.1 eV in both samples not only have similar shapes, but also similar temperature dependences. It therefore indicates that oxygen contamination also occurs in the low-concentration samples and is responsible for the extra luminescence peak. This contention is supported by the observation of some sample-to-sample irreproducibility in the intensity of this peak. It is certainly expected that oxygen contamination would be the most important in low-concentration samples because the partial pressure of SiH_4 is lowest in these samples, and the deposition rate is also very low. In the deliberately contaminated sample, the partial pressure of air was 40% that of SiH_4 . The same fraction would occur in 1% samples with a residual air pres-

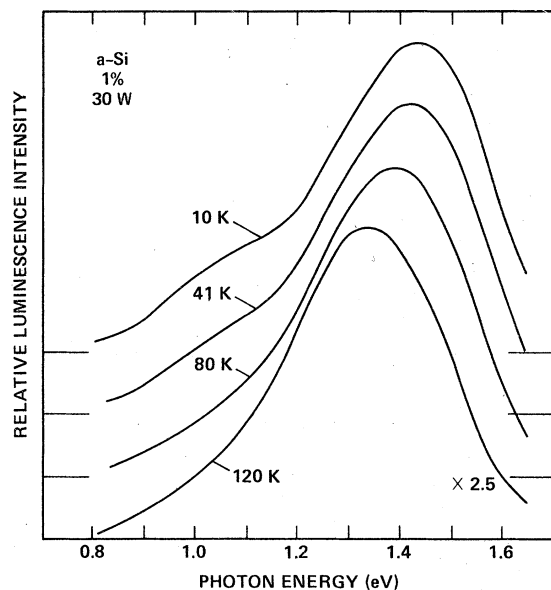


FIG. 11. Luminescence spectra of a 1% 30-W sample at various temperatures showing the relative decrease of the peak at 1.1 eV with increasing temperature.

sure of 6×10^{-4} Torr, which is within the range of values that might be anticipated from outgassing of the reactor chamber.

F. ESR measurements

ESR measurements were performed on samples prepared under various deposition conditions. In every case, where a resonance is detectable, the line shapes are identical and have a width of ~ 7 G at $g = 2.005$, in agreement with many other ESR

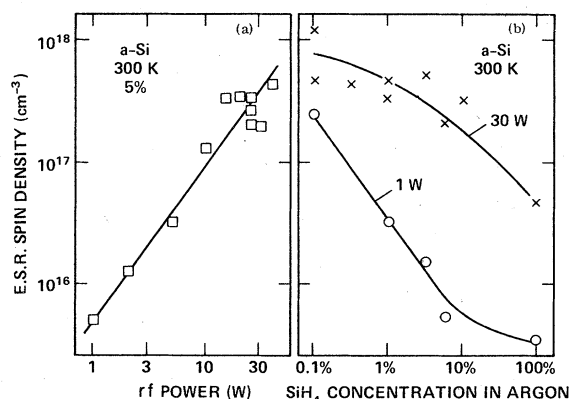


FIG. 12. (a) Dependence of the room-temperature ESR spin density on rf power for 5% samples. (b) Dependence of the room-temperature ESR spin density on silane concentration for 1- and 30-W samples.

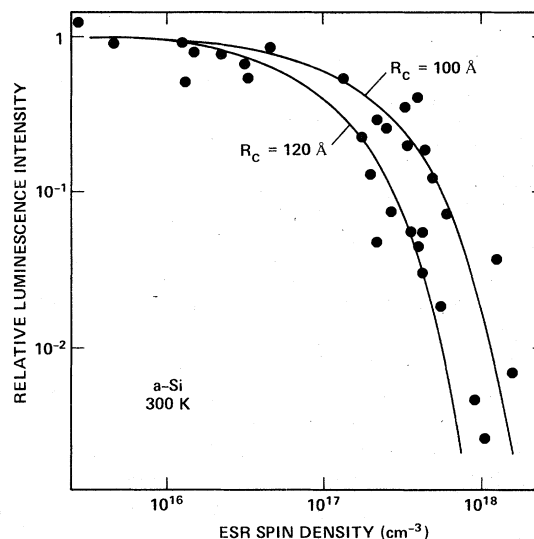


FIG. 13. Luminescence intensity plotted against ESR spin density for samples prepared under a wide variety of deposition conditions. The solid lines are fits to a model described in Sec. IV E.

measurements on *a*-Si.¹¹ Figure 12(b) shows a plot of spin density against silane concentration for 1-W and 30-W samples, and the spin density is clearly maximized at low concentration and high power. The equivalent plot of luminescence intensity given in Fig. 4 shows that there is a direct correlation between the presence of centers giving spin and the existence of a competing nonradiative transition that quenches the luminescence intensity. This correlation is also evident in the dependence on rf power shown in Fig. 12(a) which may be compared to the variation of the luminescence intensity shown in Fig. 3. The same correlation is found in samples deposited at different substrate temperatures and for samples at various bias voltages. The spin density observed through the variation of all of these parameters is plotted against the luminescence intensity in Fig. 13. Despite considerable scatter in the data, the origin of which is not yet clear, the overall correlation is again very striking and furthermore demonstrates that a single universal curve describes all the different deposition parameters. Evidently a spin density of greater than $\sim 10^{17}$ cm⁻³ results in a large decrease in luminescence intensity, whereas lower densities have a smaller effect.

ESR was also investigated in air-contaminated samples. However, no resonances in addition to the standard line at $g = 2.005$ were detected. It therefore appears that the oxygen center is either spinless or undetectable owing to a combination of low density and a broad linewidth.

IV. DISCUSSION

A. General observations

These luminescence studies find a systematic variation of luminescence intensity and spectrum with deposition conditions. Clearly, the detailed behavior of the plasma during deposition influences the structure of the films, and possible mechanisms are described in Sec. IV C. The principal luminescence peak usually occurs near 1.4 eV, with a second peak at 1.1 eV sometimes evident. The peak at 1.1 eV is associated with oxygen impurities and is discussed further in Sec. IV D. The intensity of the 1.4-eV peak is observed to correlate with the room-temperature spin density, and the largest spin densities are found in the most weakly luminescent samples. The relation between luminescence, spin density, and localized states in the gap is discussed in detail in Sec. IV E.

Previous studies have concluded that the dominant luminescence is from the recombination of electron-hole pairs that are presumed to be in band tail states¹² at the respective band edges. The luminescence has a Stokes shift of about 0.5 eV.⁸ The evidence for not associating the peak with recombination at defects is partly the fairly high luminescence energy compared to the band gap, and partly the observation that when defects are introduced, for example, by ion bombardment, the luminescence intensity decreases strongly.⁷ The conclusion is that any defect states are primarily nonradiative. This result is strongly supported by our ESR measurements of Fig. 13 since a large spin density corresponds to a large density of states in the gap. Furthermore, in the majority of luminescent materials, nonradiative transitions proceed through deep localized states. We therefore conclude that the luminescence intensity is a useful measure of the density of localized states in the forbidden gap.

A striking feature of the luminescence results is the sensitivity of the intensity to the deposition conditions even with a fixed deposition temperature. Previous investigations have shown that the luminescence is very sensitive to the deposition temperature, but have not investigated other variables. We find that it is just as important to specify the rf power and silane concentration, and that other parameters also affect the intensity. Since we conclude that the changes in luminescence intensity are the result of a variation in the localized state density, we expect that in any experiment which involves states in the gap, there will be a similar dependence on deposition parameters. Therefore, any attempt to compare the results obtained by different groups is only valid if the deposition conditions are known to be equivalent. Pos-

sibly, the spectral shape and intensity of the luminescence is a means to establish the equivalence of different samples, with the luminescence intensity providing a figure of merit to establish the relative density of states in the gap.

The effect of deposition conditions can be clearly seen by comparing the luminescence measurements of different groups. For example, Engemann and Fischer^{6,10} observe the dominant peak to be at 1.25 eV, with other lines at 1.1 and 0.92 eV. The lower energy of their main peak compared to our data may be related to the shift that is observed in biased samples shown in Fig. 9. However, even in biased samples, we are unable to reproduce the two low-energy peaks with the same substrate and annealing temperatures as used by Engemann and Fischer. (These peaks are distinguishable from the oxygen line at 1.1 eV by the line shape and the thermal quenching behavior.) Evidently the deposition conditions are not equivalent and their use of an inductively coupled deposition reactor may partially account for the difference. Spear and co-workers³ also use an inductive system. Their samples have their main luminescence peak at 1.3 eV but lower-energy peaks are not observed.¹³ On the other hand, Pankove and Carlson⁹ do report a luminescence peak at 1.44 eV, but only when depositing from SiH₄-H₂ gas mixtures. Finally, we note that silicon samples reactively sputtered in hydrogen also give luminescence spectra that are different from any so far obtained from glow discharge samples.¹⁴ The comparison of luminescence spectra demonstrates that in each case samples of differing structure have been studied. Also, it is evident that significant deposition parameters remain that are not included in this study and which must account for the luminescence peaks that we do not observe.

B. Luminescence spectral line shape and peak energy

Systematic shifts in the luminescence peak energy are observed in the data reported above. There are three main reasons why such shifts might occur. Firstly, the band gap can vary with the deposition conditions. The most obvious way for this to occur is by changing the amount of hydrogen in the films since hydrogen is expected to increase the band gap.⁵ Secondly the distribution of zero-phonon energies for the luminescence transition could change, for example, because of a change in the shape of the band tails. Finally, an increase in the electron-phonon coupling strength would broaden the spectrum and shift the peak with respect to the zero-phonon energy.

In Fig. 7, it is seen that decreasing the deposition temperature shifts the luminescence to low

energy and broadens the line shape. A similar, but smaller, effect occurs when the rf power is increased, as shown in Fig. 2(b). Optical-absorption measurements were performed on these and similar samples to determine which of the possible mechanisms is responsible for the shift. It is found that both with decreasing deposition temperature and increasing rf power, the absorption edge near 10^4 cm^{-1} moves systematically to higher energy, and the slope decreases. In the first case, the shift is $\sim 0.3 \text{ eV}$ and in the second case, $\sim 0.1 \text{ eV}$ at 10^4 cm^{-1} . If the effect on the luminescence peak energy is due to a change in either the band gap or the zero-phonon energy, then the absorption should shift to low energy, contrary to observation. We therefore deduce that in both cases the shift in the luminescence is due to an increase in the strength of the electron-phonon coupling, while the zero-phonon energy remains essentially unchanged. This effect explains the shift of the absorption edge to higher energy. Previously⁸ we have found that the absorption, at least up to $\sim 10^3 \text{ cm}^{-1}$, contains a substantial component from the same electronic transitions that are observed in luminescence. In absorption, these transitions are shifted above the zero-phonon energy by an amount dependent on the coupling strength. Thus the increased coupling in high-power samples is expected to shift the absorption edge to higher energy. From the luminescence and absorption measurements, it is estimated that the Stokes shift increases from $\sim 0.4 \text{ eV}$ in $10\% \frac{1}{2}\text{-W}$ samples to $\sim 0.5 \text{ eV}$ in $10\% \text{ 30-W}$ samples, and to $\sim 0.6 \text{ eV}$ in the low deposition temperature samples.

The increase in the electron-phonon coupling strength must presumably be related to a decrease in the rigidity of the lattice, but we cannot determine whether the change occurs equally at all band tail states, or whether the coupling strength is determined locally by specific structural configurations whose distribution is changing. However, it is interesting to note that infrared measurements¹⁵ find that as the deposition temperature decreases or the rf power increases, hydrogen tends to be incorporated in paired units (SiH_2) rather than singly (SiH), and small lengths of polysilane chains, $(\text{SiH}_2)_n$, occur. Since the chain molecule is inherently flexible, an increase in the coupling strength might be expected. A more flexible lattice might also result from an increased density of voids.

C. Plasma properties

The systematic variation in luminescence intensity and electron-spin density over the power and silane-concentration space is paralleled by well-defined variations in deposition rate. Figure 14 il-

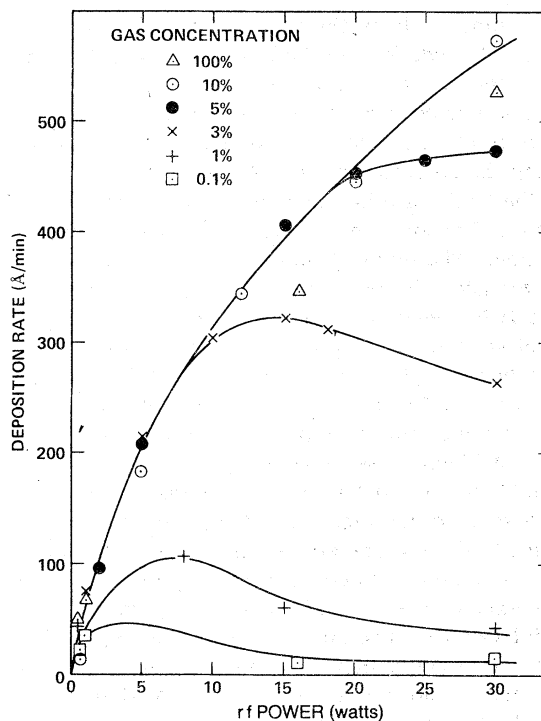


FIG. 14. Dependence of the deposition rate of α -Si films on rf power for various gas concentrations.

lustrates these variations.

At the lowest power, $\sim 0.5 \text{ W}$, the deposition rate is independent of the silane concentration to within experimental accuracy. As the power is increased, for high concentrations ($\geq 10\%$) there is a monotonic rise in deposition rate. For lower concentrations, the deposition rate diverges from this rise, peaks and then begins to decline, the onset of the deviation occurring at progressively lower power as the concentration is reduced.

We explain these observations as follows. At low power, we see that the deposition rate is not limited by the supply of silane or SiH_x radicals or ions from the plasma because it is independent of the silane concentration. Since we do not anticipate a factor of 1000 difference in the relative degrees of ionization of argon and silane, this suggests that the rate limiting process involves another plasma species, e.g., an electron, interacting with a silicon containing species adsorbed onto the deposition surface. As the power is raised, the reaction rate increases approximately linearly with power until the reaction rate is equal to the supply of the adsorbed species, at which point the deposition rate would be expected to deviate from linearity and become power independent. The observation of a declining deposition rate at high power follows from the finite distance from the gas inlet to the substrate—silane is progres-

sively removed from the gas as it moves downstream. In addition, in the arrangement shown in Fig. 1, the plasma is localized around the electrodes at low powers but extends further toward the gas inlet as the power is increased, thus amplifying the depletion effect.

On the basis of this explanation we define two regimes of deposition—silane excess and silane depletion. The former includes all combinations of power and dilution that fall on the curve followed by the 10% concentration. (For reasons that are not yet clear, the points for pure silane fall below those for 10% concentrations.) Silane depletion is defined by a deposition rate independent of or declining with power. An intermediate regime bridges these extremes.

Considering the behavior of the luminescence and ESR described earlier, it is clear that samples produced in the silane depletion regime possess many more defect states than those produced in the silane excess regime. There are, however, substantial variations in luminescence and ESR results within the silane excess regime indicating that silane excess is not the sole factor responsible for low-defect concentrations. It is also worth noting that there is no correlation between defect state densities and deposition rate, a parameter considered significant in other physical deposition processes.

Several possible explanations exist for the association of high defect state densities with silane depletion. The most straightforward is inadequate hydrogenation of dangling bonds due to a lower partial pressure of hydrogen at the surface. Preliminary attempts to identify this mechanism by addition of hydrogen to the gas have not resulted in substantial changes in luminescence intensities. However, the complexity of the plasma chemistry may not permit this type of approach and other explanations for high-defect densities, such as argon-ion bombardment, must also be considered. We conclude, therefore, that the deposition regimes described are strongly correlated with the presence of defect states in the α -Si but that further work is necessary to describe the mechanism by which these states are created.

D. Oxygen line near 1.1 eV

Oxygen contamination introduces a broad luminescence peak centered near 1.1 eV with a line width of 0.3–0.4 eV, which is also observed in low-concentration samples owing to the residual atmosphere. We assume that the radiative transition involves localized states directly associated with

oxygen atoms. The alternative possibility that oxygen is itself inactive, but introduces a silicon defect, seems unlikely, since there are many samples in which defects exist but which do not give the same luminescence line. We further expect that the active oxygen centers are not associated with oxygen in twofold coordination. It seems to be a common property of amorphous systems that an impurity that satisfies its valence requirements does not give an active center. We suggest instead that the active oxygen may be singly or threefold coordinated to Si, and that there may be a strong similarity to the D^+ and D^- centers that are postulated in chalcogenide glasses,¹⁶ since these arise from chalcogens with coordination different from two. Singly coordinated, "nonbridging" oxygen is an important defect in SiO_2 and Mott¹⁷ has already proposed that in this material the defect should behave as a D^- center. Furthermore, model calculations of oxygen on the surface of crystalline Si show that the highest filled electronic state of a threefold coordinated oxygen is at higher energy than for singly coordinated oxygen if the center is neutral, but lower if it is positively charged.¹⁸ This result is approximately the condition for charged defects to form.

Further evidence for this description of the oxygen impurity is the very striking similarities between its luminescence and that found in As-chalcogenide glasses,¹⁹ which is thought to involve D^- centers. Firstly, the width of the oxygen line indicates a strong electron-phonon interaction, although excitation spectra have not yet been measured to confirm this. Secondly, there is a similar relation between band gap, luminescence peak energy, and linewidth, as was found in chalcogenide glasses. Thus, the oxygen luminescence peak is at $\sim \frac{1}{2}E_g$ and the linewidth is about the same as for defects in As_2Se_3 or As_2S_3 . Thirdly, thermal quenching occurs at a lower temperature than for the 1.4-eV peak, despite a lower luminescence energy. In chalcogenides a similar strong thermal quenching is attributed to the charge on the defect which counteracts the Coulomb interaction of the electron-hole pair recombining at the defect,¹⁹ and possibly the same mechanism occurs in the oxygen center. Furthermore, no ESR signal characteristic of oxygen is observed in contaminated Si samples. This observation is consistent with the center being a spinless D^- or D^+ , but of course cannot exclude the presence of oxygen centers with spin if their ESR line width is sufficiently large. Finally, the interpretation is also consistent with the observation²⁰ that oxygen diffused into evaporated silicon dramatically reduces the spin density although it does not apparently change the density of defect states.

E. Relation between luminescence and ESR

The correlation between ESR spin density and luminescence intensity is established in Figs. 12 and 13 and the observation of a universal relation between these two measurements is of particular significance. This result demonstrates that a one-to-one correspondence exists between states which have spin and states which quench the luminescence, irrespective of which deposition parameter is varied. The implication is that different deposition conditions all produce the same type of defect. Thus a considerable simplification results, in which a single measurement, either luminescence intensity or spin density, seems to be a unique measure of the defect structure of the film, at least for the range of deposition conditions used in this study. It remains to be seen whether this characterization applies to other measurements.

Based on measurements of the luminescence decay time, Tsang and Street²¹ have proposed a model to relate the luminescence intensity to the defect density. They suggest that at low temperatures, band-edge electron-hole pairs are sufficiently immobile that capture by a defect occurs by tunnelling with rate $\omega_0 \exp(-2R/R_0)$, where R is the distance to the defect, R_0 is the radius of the particle that tunnels, and $\omega_0 \sim 10^{12} \text{ sec}^{-1}$. A critical transfer radius R_c is defined as the largest value of R for which tunnelling is more probable than the radiative recombination rate P_R , and is given by

$$2R_c = R_0 \ln(\omega_0/P_R). \quad (1)$$

It was then shown that for a random distribution of defects the luminescence quantum efficiency y_L is given by

$$y_L = \exp(-\frac{4}{3} \pi R_c^3 N_D), \quad (2)$$

where N_D is the defect density.

Figure 13 shows that Eq. (2) gives a good description of the data if it is assumed that N_D is proportional to the spin density N_s

$$N_D = \beta N_s. \quad (3)$$

Both the insensitivity of y_L to N_s at values below $10^{17} \text{ spins/cm}^3$ and the rapid decrease of y_L at larger N_s are explained by the model. We believe this result confirms the model²¹ of a nonradiative transition by tunnelling to defect states. From the fit to the data shown by the two solid lines in Fig. 13, we obtain

$$R_c \beta^{1/3} = 110 \pm 10 \text{ \AA}$$

Thus using values $\omega_0 = 10^{12} \text{ sec}^{-1}$ and $P_R = 10^5 \text{ sec}^{-1}$ (Ref. 21), Eq. (1) gives

$$R_0 = 12 \beta^{-1/3} \text{ \AA}.$$

Unfortunately, the value of R_0 is not accurately known, so that β cannot be obtained directly. However, for states near the Fermi energy, R_0 is often assumed to be 5–10 Å.³ Since the band tail certainly comprises shallower, and therefore more extended states, a value for R_0 of 12 Å is a reasonable assumption. Thus, the data are consistent with N_s measuring the total density of states that quench the luminescence although a value of β as large as about 5 cannot be excluded. We note that in studies of the effects of ion bombardment, a similar question of the relation between spin density and the total density of states in the gap was discussed.²² Within similar uncertainties regarding the value of various parameters, it was also found that the data could be adequately explained assuming equality between the two densities.

V. SUMMARY

The present investigation demonstrates the sensitivity of photoluminescence to deposition conditions in hydrogenated amorphous silicon produced by plasma decomposition of silane. The most important deposition variables are the substrate temperature, rf power and the concentration of silane in argon. An electrical bias at the sample surface is also significant and may be responsible for some of the differences between the luminescence properties of our samples compared to those produced in inductively coupled deposition reactors.

By varying the deposition conditions, a change in both the intensity and spectral line shape of the luminescence occurs. In some cases, absorption measurements indicate that the latter is caused by a change in the strength of the electron-phonon interaction. However, the intensity of luminescence is determined by the defect density. ESR measurements demonstrate that there is a correlation between a decreasing luminescence intensity and an increasing density of unpaired spins. We show that this relation can be explained by a model in which nonradiative transitions occur when carriers tunnel into localized defect states.

It is evident that the presence of defects with spin, and possibly the strength of the electron-phonon coupling as well, are determined by the way in which hydrogen is incorporated into the samples. We can identify two film growth regimes, which clearly affect the defect density, corresponding to surface reactions whose rate is limited either by the supply of Si-H species, or by the available power to drive the reaction. Infrared measurements¹⁵ also show that there is a correlation between luminescence properties and the bond-

ing configurations of hydrogen to silicon. It is hoped that further work in this direction will enable a structural origin for the defects to be identified.

We also observe luminescence from oxygen impurities in amorphous silicon. The oxygen is introduced by depositing samples in a low partial pressure of air. However, in some cases, notably when using very low concentrations of silane, the oxygen is also present as a native impurity. From

observations of the oxygen luminescence, we speculate that the active centers are very similar to the charged defects (D^+ , D^-) that are postulated in chalcogenide glasses.

ACKNOWLEDGMENTS

We are grateful to G. Lucovsky for valuable discussions and to R. Lujan for technical assistance in sample preparation.

-
- ¹H. Mell, in *Amorphous and Liquid Semiconductors*, edited by J. Stuke and W. Brenig (Taylor and Francis, London, 1974), p. 203.
- ²K. L. Chopra and D. K. Pandya, in *Amorphous and Liquid Semiconductors*, edited by J. Stuke and W. Brenig (Taylor and Francis, London, 1974), p. 1141.
- ³W. E. Spear, in *Amorphous and Liquid Semiconductors*, edited by J. Stuke and W. Brenig (Taylor and Francis, London, 1974), p. 1.
- ⁴M. H. Brodsky, M. A. Frisach, J. F. Ziegler, and W. A. Lanford, *Appl. Phys. Lett.* **30**, 561 (1977).
- ⁵J. C. Knights, *AIP Conf. Proc.* **31**, 296 (1976).
- ⁶D. Engemann and R. Fischer, in *Proceedings of the Twelfth International Conference on Physics of Semiconductors*, edited by M. H. Pilkuhn (Tuebner, Stuttgart, 1974), p. 1042.
- ⁷D. Engemann, R. Fischer, F. W. Richter and H. Wagner, in *Structure and Properties of Non-Crystalline Semiconductors*, edited by B. T. Kolomiets (Leningrad, 1976), p. 217.
- ⁸R. A. Street, *Philos. Mag.* **37**, 35 (1978).
- ⁹J. I. Pankove and D. E. Carlson, *Appl. Phys. Lett.* **29**, 620 (1976).
- ¹⁰D. Engemann, Ph. D. thesis (Marburg, 1975) (unpublished).
- ¹¹J. Stuke, in *Proceedings of the Seventh International Conference on Amorphous and Liquid Semiconductors*, edited by W. E. Spear (University of Edinburgh, 1977), p. 406.
- ¹²D. Engemann and R. Fischer, *AIP Conf. Proc.* **31**, 37 (1976).
- ¹³T. S. Nashashibi, I. G. Austin, and T. M. Searle, *Philos. Mag.* **35**, 831 (1977).
- ¹⁴M. H. Brodsky, J. J. Cuomo, and F. Evangelist, in *Proceedings of the Seventh International Conference on Amorphous and Liquid Semiconductors*, edited by W. E. Spear (University of Edinburgh, 1977) p. 397.
- ¹⁵J. C. Knights, G. Lucovsky, and R. J. Nemanich, *J. Non-Cryst. Solids* (to be published).
- ¹⁶R. A. Street and N. F. Mott, *Phys. Rev. Lett.* **35**, 1293 (1975); N. F. Mott, E. A. Davis, and R. A. Street, *Philos. Mag.* **32**, 961 (1975).
- ¹⁷N. F. Mott, *Adv. Phys.* **26**, 363 (1977).
- ¹⁸D. J. Chadi (private communication).
- ¹⁹R. A. Street, *Adv. Phys.* **25**, 397 (1976).
- ²⁰P. G. LeComber, R. J. Loveland, W. E. Spear, and R. A. Vaughan, in *Amorphous and Liquid Semiconductors*, edited by J. Stuke and W. Brenig (Taylor and Francis, London, 1974), p. 245.
- ²¹C. Tsang and R. A. Street, *Philos. Mag.* (to be published).
- ²²J. Stuke, in *Electronic Phenomena in Non-Crystalline Semiconductors*, edited by B. T. Kolomiets (Leningrad, 1976), p. 193.